Soft Matter

Gold nanorod impact on mechanical properties of stretchable hydrogels

Journal:	*Soft Matter*
Manuscript ID	SM-ART-04-2020-000737.R1
Article Type:	Paper
Date Submitted by the Author:	02-Jun-2020
Complete List of Authors:	Turner, Jacob; University of Illinois at Urbana-Champaign, Department of Chemistry Og, Jun; University of Illinois at Urbana-Champaign, Department of Chemistry Murphy, Catherine; University of Illinois at Urbana-Champaign, Department of Chemistry

Soft Matter

Gold nanorod impact on mechanical properties of stretchable hydrogels

Jacob G. Turner, † Jun Hyup Og, † and Catherine J. Murphy*

Department of Chemistry, University of Illinois at Urbana-Champaign, 600 S. Mathews Avenue, Urbana, Illinois 61801, United States

ABSTRACT

Double-network hydrogels have attracted much attention because of their superior mechanical properties, which are more similar to rubbers and soft tissues than classic hydrogels. In this report, plasmonic gold nanorods (AuNRs) are incorporated into a stretchable double-network hydrogel, composed of alginate and acrylamide. The impact of gold nanorod concentration and surface chemistry on bulk mechanical properties such as Young's modulus and elongation at break was investigated. AuNRs with three different surface chemistries, cetyltrimethylammonium bromide, thiolated poly(ethylene glycol), and 11-mercaptoundecanoic acid were successfully dispersed into alginate/polyacrylamide hydrogels. The AuNR-loaded hydrogels could be reversibly stretched, leading to AuNR reversible alignment along the stretch direction as judged by polarized optical spectroscopy. With the proper surface chemistry, hydrogel nanorod composites were able to be stretched to more than 3,000% their initial length without fracturing. These results show that plasmonic gold nanorods can be well dispersed in multi-component polymer systems, certain surface chemistries can enhance the bulk mechanical properties, and AuNR orientation can be controlled through varying strains on the matrix.

Soft Matter

1. INTRODUCTION

In the last 15 years, hydrogels have become extensively studied materials because of their biocompatibility, stimuli-responsiveness, and swelling/deswelling properties, among others.[1-3] Hydrogels are soft materials that consist of three-dimensional crosslinked polymer networks dispersed in high amounts of water (above 50 wt%) useful for waste treatment, tissue engineering, biosensing, and show promise in areas such as wearable electronics.[2,4-8] More recent advances in engineering hydrogels have been made to further enhance their properties and make them extremely tough, conductive, and/or self-healable.[1,8-12] Among these advanced hydrogels, double-network hydrogels have shown extraordinary mechanical properties making them ideal materials for tissue engineering and flexible electronics.[3] These mechanical properties include high fracture energies, high stretchability, and high modulus, all of which are comparable to that of tendons, ligaments, and rubbers.[1,3]

Adding nanomaterials as fillers to polymer composites to enhance materials is common practice. The auto-industry has added nanoparticle clays to strengthen materials for decades.[13] Nanomaterials such as ZnO nanorods, carbon nanotubes, and gold nanoparticles have been successfully dispersed into polyurethanes to provide advanced properties such as conductivity and shape-memory.[14-16] Control over nanoparticle orientation and assembly in polymer composites is challenging, especially in multi-polymer systems.[13] It has been shown that gold nanorod (AuNR) alignment can be controlled by the strain of stretchable materials, these examples embed or disperse the AuNRs in polymer films.[17-21] Understanding how nanoparticles behave in multi-polymer 3D systems is not well understood. In particular, the behavior of nanorods in 3D polymer networks is not as well studied as nanospheres and nanowires.

Soft Matter

Understanding the impact of anisotropic nanoparticle fillers on double network hydrogels will be important for future material development.

Many hydrogels have nanomaterials incorporated into them (nanocomposite hydrogels) to help make them conductive, reinforce the mechanical properties, or make them antibacterial.[22-25] Plasmonic nanoparticles are of particular interest because of their strong light absorption and scattering. Among plasmonic nanoparticles, gold nanorods (AuNRs) are unique because their longitudinal plasmon can be tuned from the visible portion of the electromagnetic spectrum to the near-infrared by changing the aspect ratio of the AuNR.[26,27] Previously, gold nanoparticles have been incorporated into hydrogels for protein detection, as an extra-cellular matrix mimic, drug delivery, cardiac tissue engineering, and to give hydrogels optical and thermal responsiveness.[28-36] Stretchable plasmonic materials have been created, but the stretchable substrate is often an elastomer which lacks the biocompatibility and stimuli-responsiveness of hydrogels.[37-39] Stretchable hydrogels present a unique opportunity to create biocompatible stretchable plasmonics that can be used for wearable electronics, bio-sensors, and optical devices. Another advantage of hydrogels is their dispersion medium is water, so a variety of NP surface chemistries can be introduced into the pre-gel solution. Therefore advanced surface modifications to make the AuNRs well dispersed is not necessary as in other polymer composites.[21,40]

In this report, AuNR hydrogel composites were synthesized where the hydrogel matrix is a double network with alginate and acrylamide (AAm), which itself can be stretched reversibly to more than twenty-times its initial length.[10,41] The Na-alginate/PAAm hydrogels can be ionically crosslinked with Ca^{2+} to yield a much tougher hydrogel compared to Na-alginate/PAAm hydrogel.[10,41] The AuNRs were incorporated into the pre-gel solution and stayed

Soft Matter

well dispersed throughout the curing process. The Na-alginate/polyacrylamide (PAAm) stretchable hydrogels align the AuNRs along the stretch direction when elongated. Because the AuNRs were incorporated into the pre-gel solution before polymerization and crosslinking, the influence of AuNR surface chemistry and concentration have on the mechanical properties of these hydrogels was also studied. These properties were investigated as a function of surface chemistry for three different common surface chemistries for AuNRs: cetyltrimethylammonium bromide (CTAB), thiolated poly(ethylene glycol) (PEG-SH), and 11-mercaptoundecanoic acid (MUA). For the non-ionically crosslinked hydrogels (Na-alginate/PAAm) the Young's modulus is dependent on AuNR concentration, but for ionically crosslinked hydrogels (Ca-alginate/PAAm) the Young's modulus is dependent on AuNR concentration and surface chemistry.

2. MATERIALS AND METHODS

2.1 Materials and Instrumentation

Chloroauric acid ($HAuCl_4 \cdot 3H_2O$, 99.9%), cetyltrimethylammonium bromide (CTAB, 99%), silver nitrate ($AgNO_3$, 99%), hydroquinone (99%), sodium borohydride ($NaBH_4$, 99%), 11-mercaptoundecanoic acid (MUA, 95%), sodium alginate, acrylamide (98%), ammonium persulfate (APS, 98%), N,N'-methylenebisacrylamide (MBAA, 99.5%), N,N,N',N'-tetramethylethylenediamine (TEMED, 99%) were purchased from Sigma-Aldrich. Sodium hydroxide (NaOH, 98%) was purchased from Fisher Scientific. Thiolated poly(ethylene glycol) (PEG-SH, M.W. 5,000) was purchased from NANOCS. Ethanol (200 proof) was purchased from Decon Laboratories Inc. and used without purification. All water used was DI water purified by a Barnstead Nanopure II purification system (>17.8 MΩ).

Soft Matter

Transmission electron microscopy (TEM) of AuNRs was performed using a JEOL 2010 LaB_6 or JEOL 2100 Cryo LaB_6. TEM of hydrogels was done using a Hitachi Hg00 microscope. All nanorod sizing was done using ImageJ and a minimum of 300 nanorods were measured. A Nicolet Nexus 670 spectrometer equipped with a germanium crystal plate was used for ATR-FTIR measurements. Zeta potentials were measured using a Malvern Zetasizer Nano ZS instrument. All Young's modulus results were obtained using a Q800 Dynamic Mechanical Analyzer (DMA). Maximum elongation tensile testing measurements were done using a 1 kN MTS Insight 2 with a 250 N load cell. UV-vis spectra were obtained using a Cary 5000 UV–vis–near-infrared spectrophotometer. For polarized measurements a 5 mm circular aperture was used, along with a Glan-Thompson polarizer.

2.2 Synthesis of Gold Nanorods

Gold nanorods were prepared using a seed-mediated method with hydroquinone as the reducing agent.[42] To synthesize the CTAB-capped gold seeds a vial was prepared with 9.5 mL of 0.10 M CTAB and 0.5 mL of 0.10 M $HAuCl_4 \cdot 3H_2O$ was added. While this seed solution was stirred vigorously, 0.460 mL of freshly prepared, ice-cold $NaBH_4$ in 0.010 M NaOH was injected rapidly into the seed solution. The seed solution color became dark brown immediately following the addition of $NaBH_4$. The seeds were aged at room temperature without stirring for 1 hour before use. To prepare enough seeds for the typical 1 L AuNR growth solution, two identical batches of seeds were made. For a 1 L batch of AuNRs, a growth solution was prepared by adding 950 mL of 0.10 M CTAB to a large flask, followed by the addition of 1.30 mL of 0.10 M $AgNO_3$ and 50 mL of 0.010 M $HAuCl_4$, with gentle stirring. Then, 50 mL of 0.10 M hydroquinone was added; the solution was stirred until it was nearly colorless. Next, 16 mL of CTAB-capped gold seeds (aged for 1-4 hours) was added to the growth solution, which was then

Soft Matter

stored at 27° C with mild stirring for 12-18 hours. The AuNRs were purified by centrifugation at 8,000 rcf for 20 min. The supernatants were discarded and the AuNR pellets were redispersed in nanopure water and stored at room temperature for future use. For a typical synthesis the AuNRs had an aspect ratio of 3.1 ± 0.4, with a length of 82 ± 8 nm and a width of 27 ± 3 nm.

2.3 Gold Nanorod Surface Modifications

Three surface chemistries were studied: CTAB, PEG-SH, and MUA. The procedure used for this surface modifications were adapted from a previous report.[43] The as synthesized gold nanorods are CTAB-capped and they were used after one additional wash by centrifugation at 8,000 rcf. To exchange the CTAB with PEG-SH, 1 mL of 50 mg/mL PEG-SH was added to 40 mL of 1 nM CTAB capped AuNRS (twice centrifuged). The AuNRs were then gently shaken overnight using a mechanical shaker and then purified by two rounds of centrifugation at 8,000 rcf for 30 minutes. These PEG-SH modified AuNRs can be further functionalized by replacing the thiolated polymer with shorter chain thiols, such as MUA.[44] For this process, 2 mL of 0.10 M NaOH were added to 40 mL 1 nM PEG-SH modified AuNRs and then 4 mL of 20 mM MUA dissolved in ethanol was subsequently added. The AuNRs were gently shaken overnight on a mechanical shaker and were then washed twice with water and centrifugation at 8,000 rcf for 30 minutes. The 2 mL of 0.10 M NaOH was added back in after each wash to ensure stability. Characterization data for the AuNR can be found in the Supporting Information: TEM Images (Figure S1), and ζ-potentials (Figure S2).

2.4 Synthesis of Alginate/Acrylamide Hydrogels with and without Gold Nanorods

To synthesize our dual network hydrogels we adopted a procedure from Suo and co-workers.[10,41] First, a series of stock solutions were prepared. A stock solution of 1:6 wt ratio of alginate to acrylamide was prepared by dissolving 2.325 g of alginate and 13.953 g of acrylamide in 80 mL

Soft Matter

of nanopure water (83.1 wt%, stirred overnight to dissolve). An ammonium persulfate stock solution was prepared by dissolving 0.0237 g of ammonium persulfate in 5.0 mL of nanopure water. A N,N'-methylenebisacrylamide stock solution was prepared by dissolving 0.0167 g in 10 mL of nanopure water. Once the stock solutions were prepared, they were mixed together in amounts dependent on the total water content desired, where the total water content ultimately controls the hydrogel thickness.

For a typical hydrogel synthesis, our total water content was 6.25 mL. To synthesize the hydrogels, 5.0 mL of the alginate/acrylamide stock solution was added to a small beaker and it was stirred. Then 0.625 mL of additional nanopure water was added, followed by the addition of 0.3125 mL of MBAA (acrylamide crosslinker), 0.3125 mL of APS (thermo-initiator), and 2.81 μL of TEMED (crosslinking accelerator). The resulting solution was stirred for 10 minutes before being poured into our glass mold (60 x 15 mm glass petri dish). The petri dish was covered and placed in a drying oven at 70° C for 1 hour to cure. Once cured the glass mold was removed from the oven and placed in a humid box. The above amounts lead to the desired hydrogel with 86 wt% water, 2 wt% alginate, and 12 wt% acrylamide. Relative to acrylamide monomer the amount of MBAA, APS, and TEMED were 0.028 mol%, 0.053 mol%, and 0.153 mol%, respectively. ATR-FTIR was used to structurally characterize the resulting hydrogel, shown in Figure S3.

The protocol used for synthesizing hydrogels with AuNRs is the same procedure outlined above, except instead of adding 0.625 mL of nanopure water, 0.625 mL of a AuNR solution was added, which leads to a 10-fold dilution of the AuNRs. For example, if 0.625 mL of 10 nM CTAB-capped AuNRs were added, the resulting hydrogel would have 1 nM of CTAB-capped

Soft Matter

AuNRs incorporated into its network, or about 0.03 wt%. Photographs of representative as synthesized hydrogels are shown in Figure S4.

2.5 Ca^{2+} Crosslinking of Alginate

To crosslink the alginate polymers, we followed a procedure by Suo and co-workers where they describe the strengthening of alginate/acrylamide hydrogels through multivalent cation exchange.[41] We used $CaCl_2$ as the source of Ca^{2+} to strengthen our hydrogels by first carefully removing the hydrogels from the glass petri dish and placing them in a 100 x 15 mm plastic petri dish. Then 30 mL of 0.3 M $CaCl_2$ was added to fully submerge the hydrogels in the solution, and the hydrogels were soaked for 3 hours. Afterwards the $CaCl_2$ was poured out, the hydrogels were rinsed off, and placed back into a humid box.

2.6 Mechanical Testing

The as synthesized, circular hydrogels had to be cut into pieces that could be used for mechanical testing. Each hydrogel had four or five rectangular pieces cut out of it all with the approximate dimensions of 40.0 mm long, 7.0 mm wide, and 2.0 mm thick. The hydrogel samples were kept in a humid box except for when they were being cut, measured, and tested.

To determine the Young's modulus these hydrogel pieces were tested using a Q800 DMA with a preload force of 0.0005 N and a ramp rate of 0.04 N/min. The initial gage length was measured by the instrument and each sample was stretched to 100-200% strain. The linear portion of 0-10% strain was then used to determine the Young's modulus of each sample.

A 1 kN MTS Insight 2 was used to determine the maximum elongation length because DMA has a limited achievable displacement. For these measurements the preload force was 0.01 N and the stretch rate was 100 mm/min. The initial gage length for each sample was manually measured before the test was started. The instrument does not consider the cross-sectional area of

Soft Matter

the sample when reporting stretch length, so the stretch axis was normalized to reflect the small differences in cross-sectional areas between samples. This graph was then used to calculate the maximum elongation length for each sample, where the maximum elongation length is the point at which the hydrogel fractured or reached the maximum instrument displacement.

2.7 Polarized UV-vis Measurements

Polarized UV-vis measurements were performed to determine if the AuNRs aligned when stretched. For the setup of these measurements a polarizer was inserted between the light source and the sample. The hydrogel sample was then attached to a 5 mm circular aperture by taping it down, either unstretched or stretched a certain degree. In order to isolate the AuNR extinction spectra and eliminate other contributing sources of absorbance, a baseline was first taken with just the aperture inserted and no sample. Polarized measurements were taken with a hydrogel that was not loaded with AuNRs, the spectra obtained from these measurements were then subtracted with the corresponding polarization angle of their hydrogel counterpart that was loaded with AuNRs. Images of the experimental setup are shown in Figure S5.

2.8 TEM of Hydrogels Containing AuNRs

Small pieces of the hydrogel were cut and placed into a petri dish, either stretched or unstretched. They were then exposed to osmium tetroxide vapors for 1.5 hrs. The samples were dehydrated in 10-minute ethanol dispersions with increasing concentrations (50%, 75%, 95%, and 100%). The 100% ethanol step was lengthened to overnight and then to 2 days at 4 °C. With the hydrogel now harder, it was cut into smaller pieces using a razor blade. The unstretched samples were cubed and the stretched samples were cut into thin slices to maintain the stretch direction. Thee samples were then infiltrated with LR White resin with a short acetonitrile rinse step between the ethanol series and the resin. The resin infiltration was done overnight at room temperature. The

Soft Matter

blocks were then hardened at 60 °C for 3 days. The resin does not harden when exposed to air, so a silicon embedding mold was used and an Aclar sheet was placed over hole openings to make the mold air tight. The resulting blocks were trimmed and sectioned into samples with 100-150 nm thickness using a diamond knife. The samples were then imaged with a Hitachi H600 electron microscope using an accelerating voltage of 75 kV.

3. RESULTS AND DISCUSSION

3.1 Preparation of Stretchable Plasmonic Hydrogels

Soft Matter

The alginate/PAAm hydrogel matrix was chosen because of its stretchiness and relative

Soft Matter

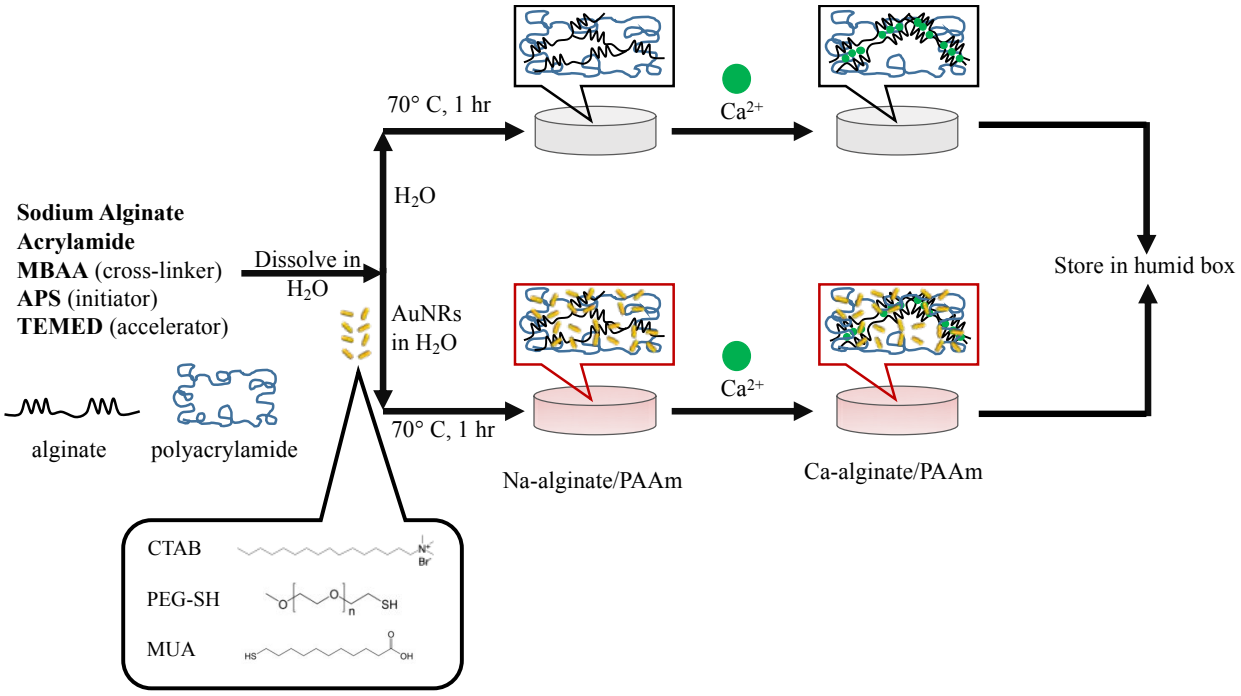

Figure 1: Illustration of the synthesis of Na-alginate/PAAm and Ca-alginate/PAAm hydrogels with and without gold nanorods (Figure not drawn to scale). The gold nanorods were incorporated into the pre-gel mixture and stay well dispersed throughout the curing and polymerization processes. The chemical structures of the three surface chemistries used are depicted. Hydrogels were stored in a humid box until they were used for testing.

ease of synthesis in aqueous solution, making it compatible for the incorporation of water-dispersible nanoparticle fillers, such as AuNRs. The hydrogels were synthesized according to the procedure outline by Yang and co-workers, with only slight modifications to incorporate AuNRs into the matrix.[10,41] Stock solutions were prepared of each reagent: alginate and acrylamide, N,N'-methylenebisacrylamide (MBAA, crosslinker), ammonium persulfate (APS, initiator), and N,N,N',N'-tetramethylethylenediamine (TEMED, accelerator). These stock solutions were all prepared in slightly higher concentrations than desired for the final hydrogel; therefore, additional water was added before curing to yield the desired hydrogel that was 86 wt% water, 2 wt% alginate, and 12 wt% acrylamide. AuNRs were incorporated by replacing the added water with a solution containing AuNRs in the pre-gel solution. An illustration of the synthesis process is shown in Figure 1.

Soft Matter

The AuNRs used in these experiments were synthesized by the method developed by Zubarev and co-workers.[42] The AuNRs had a longitudinal plasmon near 800 nm, with an aspect ratio of about 3. These were chosen because the plasmon is in the NIR window, and the length of the AuNRs is around 80 nm. Four different concentrations of AuNRs were studied; the hydrogels were synthesized so the concentration of AuNRs inside each hydrogel was 0.1 nM (about 0.003 wt%), 0.5 nM (about 0.015 wt%), 1.0 nM (about 0.03 wt%), and 2.0 nM (about 0.06 wt%). Photographs of representative as synthesized hydrogels are shown in Figure S5. These concentrations were chosen because they give the hydrogels an optical density that is suitable for absorbance based spectroscopic measurements.

Soft Matter

To strengthen the hydrogels, divalent and trivalent cations can be used to cross-link the alginate chains.[41] As the dispersion of nanomaterials into a polymer matrix is affected by nanomaterial surface chemistry, three different surface chemistries were studied: CTAB, which forms a bilayer on the gold nanorod surface and yields a net positively-charged surface coating in aqueous solution, PEG-SH, which leads to near-neutral surfaces, and MUA, which yields a net negatively-charged surface coating in aqueous solution.[26,44-45]All surface chemistries produced hydrogel composite materials in which the AuNRs were well-dispersed, unlike other pairings of AuNRs in various polymers.[40] A comparison of the AuNR solution UV-vis and the UV-vis spectra of the AuNRs dispersed in hydrogels is shown in Figure 2. The spectra of the AuNRs in the hydrogel are slightly red-shifted and broadened compared to the solution spectra of the AuNRs. This indicates a small degree of aggregation, whereas far more significant broadening and red-shifting would be expected for a large amount of aggregation.

3.2 Mechanical Properties of Stretchable Plasmonic Hydrogels

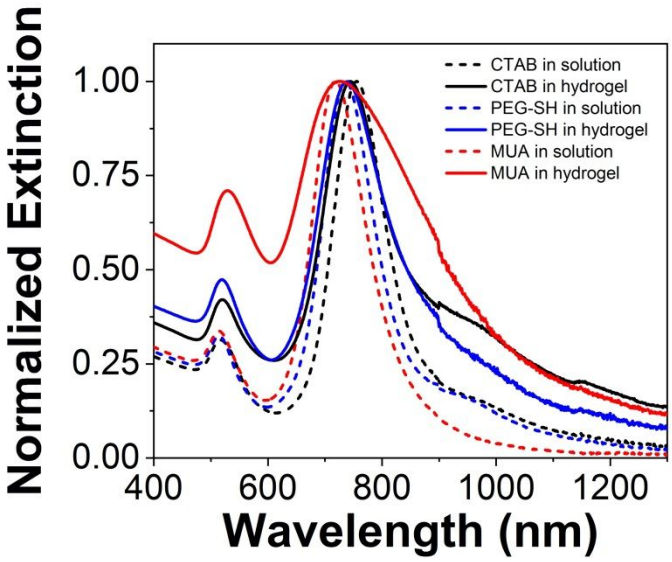

Figure 2: Normalized UV-vis spectra of AuNRs with differing surface chemistry in solution (dotted lines) and in a Na-alginate/PAAm hydrogel (solid lines).

Soft Matter

For mechanical testing, the synthesized hydrogels were cut into rectangular pieces measuring around 40.0 mm long, 7.0 mm wide, and 2.0 mm thick. Dynamic mechanical analysis (DMA) was used to determine the Young's modulus of each hydrogel. The Young's modulus, or linear tensile modules was determined from the initial slope of the stress versus strain curve in the 0-10% strain region. For the testing, at least 2 replicate hydrogels were tested with a minimum of 4 individual rectangular test samples cut from each hydrogel.

The average Young's modulus obtained for the Na-alginate/PAAm hydrogels is shown in Figure 3A. The modulus was only dependent on AuNR concentration for the Na-alginate/PAAm hydrogels; the surface chemistry of the AuNRs did not impact the modulus results as seen in Figure 3A. The averaged stress versus strain curves of the Na-alginate/PAAm for the MUA AuNR hydrogels is shown in Figure 3B, where the solid lines represent the average curve and

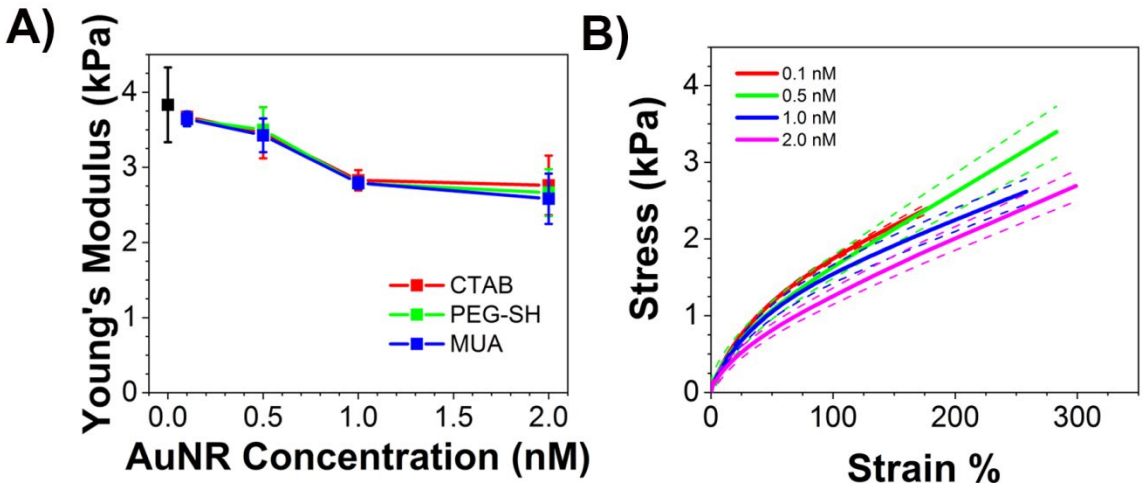

Figure 3: DMA results for Na-alginate/PAAm hydrogels with and without AuNRs of varied concentrations and surface chemistries. (A) Average Young's modulus results for each AuNR concentration and surface chemistry. (B) Averaged stress versus strain curves for MUA AuNR Na-alginate/PAAm hydrogels. The solid line is the average of multiple curves and the dotted lines are the standard error in the average curve.

Soft Matter

the dashed lines are the standard deviation in that average. Figure S6 shows the averaged stress versus strain curves for the hydrogels with CTAB and PEG-SH AuNRs.

Comparing the concentrations of just one surface chemistry (PEG-SH), at low concentrations (0.1 nM and 0.5 nM) the modulus is 3.64 ± 0.09 kPa and 3.5 ± 0.3 kPa. Compared to the modulus of the hydrogels without AuNRs, 3.8 ± 0.5 kPa the PEG-SH modulus values are not significantly different ($p > 0.05$). However, at higher concentrations of AuNRs (1.0 nM and 2.0 nM), the modulus decreased to 2.79 ± 0.5 kPa and 2.6 ± 0.3 kPa. This decrease in modulus is more than 25% and is statistically significantly lower ($p < 0.05$) than the hydrogels without AuNRs and the hydrogels with low concentrations of AuNRs. This same trend is observed for both CTAB and MUA AuNRs as well. The full tabular results of the Na-alginate/PAAm Young's modulus values, their standard deviations, and their statistical significance can be found in Table S1 and Table S2.

Nanoparticles often show very little impact on Young's modulus in polymer composites, or will even increase the modulus.[46,47] The AuNRs occupy a large volume, relative to molecular species, and are incorporated before polymerization; thus, the observed decrease in modulus is likely a result of the AuNR concentration reaching a point where it starts to impact the crosslinking density of acrylamide.[24,48] As the AuNR are concentrated enough to impede the density of acrylamide crosslinks, the material becomes less stiff, thus the modulus is lowered.

The DMA measurement is limited in its axial displacement, so it is not capable of stretching these hydrogels far enough to fracture them. To determine the maximum elongation length of hydrogels containing AuNRs, a tensile strength instrument (1 kN MTS Insight 2) was used, equipped with a 250 N load cell. With this instrument the hydrogels could be stretched far enough to determine the elongation amount before fracture. Due to the slight differences in

Soft Matter

sample size, the elongation amount was normalized by the cross-sectional area of each sample to give the most accurate comparison of results, these results are shown in Figure 4. The individual stress versus elongation curves for all hydrogel samples tested can be found in the Supplementary Information (Figures S7 through S10). The maximum elongation corresponds to how far the hydrogel was stretched before fracture or, in the case of many of the MUA AuNR hydrogels, because it reached the maximum displacement of the instrument. The values and statistical significance of the maximum elongation can be found in Table S1. For these results we observe the maximum elongation length achievable does have some dependence on AuNR surface chemistry. AuNRs with CTAB and PEG-SH and no significant difference in their elongation amount compared to the hydrogels without AuNRs ($p > 0.05$). However, the MUA AuNRs significantly enhanced the hydrogels ability to stretch, even at low AuNR concentration. Hydrogel samples with MUA AuNRs did not fracture before reaching the maximum

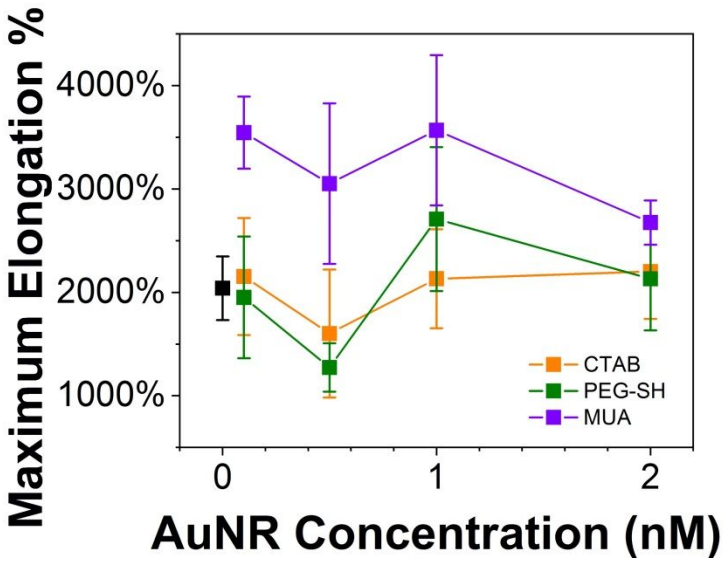

Figure 4: Maximum elongation results for each AuNR concentration and surface chemistry. The maximum elongation percentage is the percentage the hydrogel sample was stretched compared to its initial length before the sample fracture or reached the maximum displacement of the instrument (about 4,000%).

Soft Matter

displacement of the tensile instrument, more than 3,500% their initial length. It is surprising the nanorod surface chemistry makes such a measurable difference in mechanical properties of the nanocomposites. We posit that this is a result of both the hard nature of the nanorods compares to the hydrogel matrix as well as electrostatic interactions between the anionic MUA surface groups and the sodium cation crosslinking groups. Similar impact on mechanical properties have been shown for hydrogels with anionic cellulose nanocrystals.[49] These results indicate the influence surface chemistry of nanoparticle fillers can have on bulk hydrogel properties, such as their mechanical properties. Consideration of nanoparticle shape, size, and surface chemistry are important considerations for future applications.

Interestingly, when the hydrogels were ionically crosslinked with calcium, the AuNR surface chemistry impacts the modulus results as well as the AuNR concentration (Figure 5). The surface chemistry of the AuNR does not have a significant impact at low concentrations. For all of the 0.1 nM hydrogel samples there was no significant difference between them and then the

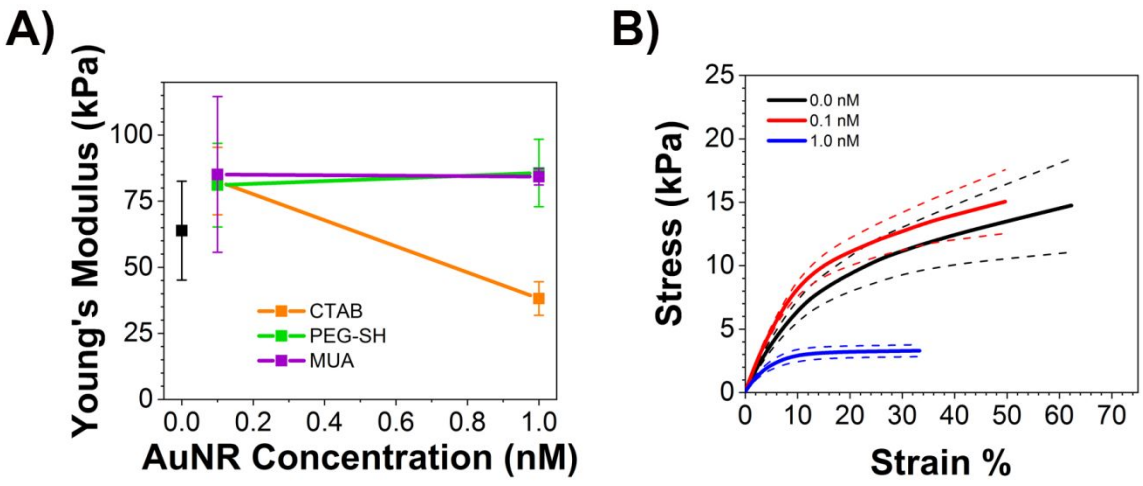

Figure 5: DMA results for Ca-alginate/PAAm hydrogels with and without AuNRs of varied concentrations and surface chemistries. (A) Average Young's modulus results for each AuNR concentration and surface chemistry. (B) Averaged stress versus strain curves for CTAB AuNR Ca-alginate/PAAm hydrogels. The solid line is the average of multiple curves and the dotted lines are the standard error in the average curve.

Soft Matter

hydrogel without AuNRs ($p > 0.05$). When the concentration of AuNRs in the hydrogels is increased to 1.0 nM, the Young's modulus for the CTAB AuNR hydrogel decreases significantly ($p < 0.05$). The average of the MUA AuNR hydrogel changes very slightly, but with much more sample consistency, the MUA Young's modulus is statistically higher than the hydrogel without AuNRs ($p < 0.05$). The average Young's modulus values and standard deviation can be found in Table S3. The averages stress versus strain curves for hydrogels containing PEG-SH and MUA AuNRs is shown in Figure S10. Elongation studies for the Ca-alginate/PAAm hydrogels with AuNRs were difficult to execute due to substantial necking in the hydrogel while stretching.

This result can be rationalized by considering the crosslinking chemistry: divalent calcium ions crosslink the acid groups in the alginate chains. The addition of an acid-containing AuNR ought to act as another "chain" in the hydrogel that can participate in the crosslinking, thus increasing the Young's modulus. In contrast, a larger dose of cationic CTAB-containing AuNRs to the hydrogel might interfere with the calcium-alginate crosslinks, if the quaternary ammonium group of CTAB ion-pairs with the alginate acid groups. This could explain why the higher loadings of CTAB-AuNRs in the hydrogels decreases the Young's modulus.

3.3 Reversible Nanorod Alignment

The plasmonic properties of AuNRs become polarization dependent when they are aligned in the same direction.[19,27,50] It has been shown that with stretchable substrates, AuNRs can orient themselves to be aligned along the stretch direction.[17-21] To measure AuNR alignment in hydrogels, a setup was devised (Figure S5). Briefly, a polarizer was inserted between the sample and the light source. The hydrogel was then attached, either stretched or unstretched, to a 5 mm circular aperture plate. Polarized measurements were taken at 0, 45, and 90 degrees, where 0 degrees is parallel to the stretch direction and 90 degrees is perpendicular. To isolate the

Soft Matter

localized surface plasmon resonance (LSPR) signals of the AuNRs and mitigate the contributing absorbance from the hydrogel, a blank hydrogel without any AuNRs was subtracted from all spectra.

Soft Matter

Figure 6A illustrates the UV-vis spectra of an unstretched hydrogel at different polarization angles. There is no polarization dependence, indicative of random orientation of the AuNRs. Figure 6B shows the same sample at the same polarization angles, but this hydrogel has been stretched 500% of its initial length. The UV-vis spectra in Figure 6B of the stretched hydrogel show the plasmon intensity change consistent with AuNR alignment. When light is polarized 0° (red), parallel to the stretch direction, the longitudinal plasmon near 746 nm remains

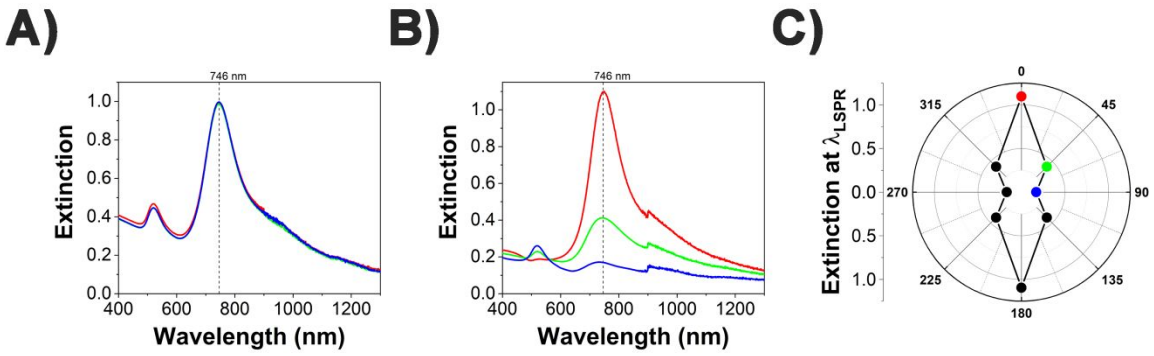

Figure 6: Polarized UV-vis on a Na-alginate/PAAm hydrogel with 1.0 nM CTAB AuNRs., where 0° is parallel to the stretch direction and 90° is perpendicular to the stretch direction. (A) Polarized UV-vis spectra at three different angles; 0° (red), 45° (green), and 90° (blue) for an unstretched hydrogel with AuNRs. (B) Polarized UV-vis spectra at three different angles; 0° (red), 45° (green), and 90° (blue) for a hydrogel with AuNRs stretched 500% its initial length. (C) Radial plot of the maximum absorbance at the longitudinal plasmon for each polarization angle for a stretched hydrogel with AuNRs.

unchanged, but the transverse plasmon intensity near 530 nm is diminished. When light is polarized 90° (blue), perpendicular to the stretch direction, the longitudinal plasmon intensity decreases significantly and the transverse plasmon increases. Figure 6C represents the change in intensity of the longitudinal plasmon mode in a radial plot of the maximum extinction at the plasmon for each polarization angle tested. These results indicate the AuNRs are being aligned along the stretch direction when the hydrogel is elongated.

Soft Matter

The AuNR alignment was further investigated by determining how the elongation amount influenced the AuNR alignment. This was done by continually stretching a single hydrogel sample further and taking polarized UV-vis measurements at each point. We monitored the degree of alignment by measuring the ratio of the maximum extinction at the longitudinal plasmon for the parallel spectrum divided by the maximum extinction at the longitudinal plasmon for perpendicular spectrum. The larger this ratio is, the more aligned the AuNRs are along the stretch direction. As shown in Figure 7, once the hydrogel has been stretched roughly 400% of its initial length the extinction ratio begins to level off and the AuNRs are fully aligned along the stretch direction. The results depicted in Figure 7 is a representative example of the 1.0 nM CTAB AuNR hydrogel. The UV-vis spectrum for each polarization angle at each elongation

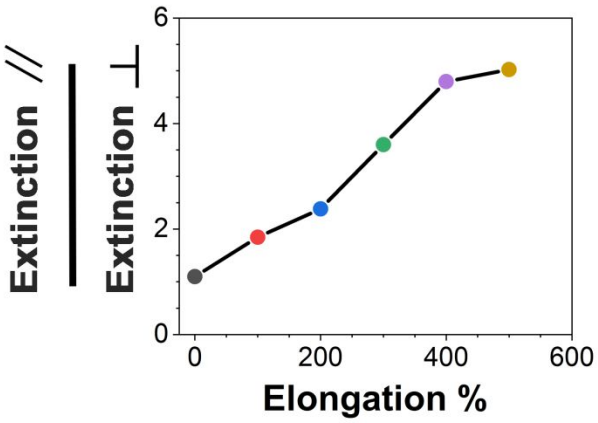

Figure 7: Plot of the ratio of the extinction at the longitudinal plasmon for light polarized parallel over light polarized perpendicular as measured by UV-vis versus the stretch % of a Na-alginate/PAAm hydrogel with 1.0 nM CTAB AuNRs. The AuNRs are becoming more aligned along the stretch direction as the hydrogel is stretched further indicated by the increasing ratio of the plasmon extinction. Colors represent different stretch percentages in relation to the initial length of the hydrogel (black: 0%, red: 100%, blue: 200%, green: 300%, purple: 400%, and gold: 500%).

% is shown in Figure S12.

Soft Matter

Notably, this AuNR alignment is also reversible. When a stretched hydrogel was returned to its relaxed state, the AuNRs were no longer aligned indicated by the lack of polarization dependence. A hydrogel with AuNRs was stretched (500% its initial length) and relaxed through three cycles, with polarized UV-vis measurements collected at each position (Figure 8). The results shown in Figure 8 are representative of a single hydrogel's alignment reversibility. The slight discrepancies in the ratios of the stretched samples is mainly due to the manually stretching of the hydrogel sample. When stretched manually, the polarizer may not be exactly perpendicular to the stretch direction, which results in a spectrum where the longitudinal plasmon is not as diminished as when the polarizer is perfectly perpendicular; this leads to a lower extinction ratio. The corresponding UV-vis spectrum for each stretch cycle is shown in Figure S13. This reversible alignment was demonstrated for different AuNR concentrations and

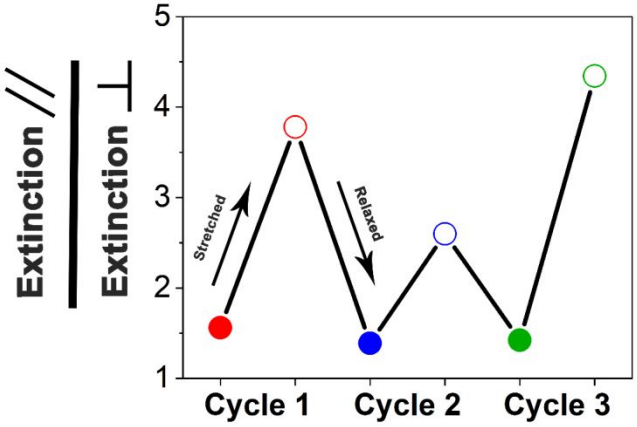

Figure 8: Plot of the ratio of the extinction at the longitudinal plasmon for light polarized parallel over light polarized perpendicular as measured by UV-vis versus the stretch/relax cycle of a Na-alginate/PAAm hydrogel with 0.1 nM CTAB AuNRs. The AuNRs are aligned when stretched indicated by the increasing ratio, and then the alignment is reversed when the hydrogel is relaxed. Colors represent different stretch/relax cycles, while filled circles represent the ratio the relaxed hydrogel, and open circles represent the ratio of the stretched hydrogel.

Soft Matter

surface chemistries and is shown in Figure S14 through S18. This result implies that the nanorods must be near the polymer chains of the hydrogel, and not trapped in water pockets.

To further confirm the AuNR alignment, transmission electron micrographs were taken of both an unstretched and a stretched hydrogel sample with 2.0 nM PEG-SH AuNRs dispersed in the hydrogel. To image the hydrogel the samples were embedded in an acrylic resin, LR White. Imagining the embedded hydrogel sample with an accelerating voltage of 75 kV, visual evidence of AuNR alignment was obtained as shown by Figure 9B. Long range ordering of the AuNRs orienting their longitudinal axis along the stretch direction of the hydrogel was observed. An image of an unstretched hydrogel is shown in Figure 9A, for an unstretched hydrogel no directional orientation of the AuNRs was observed. More images of the AuNR alignment are shown in Figure S19.

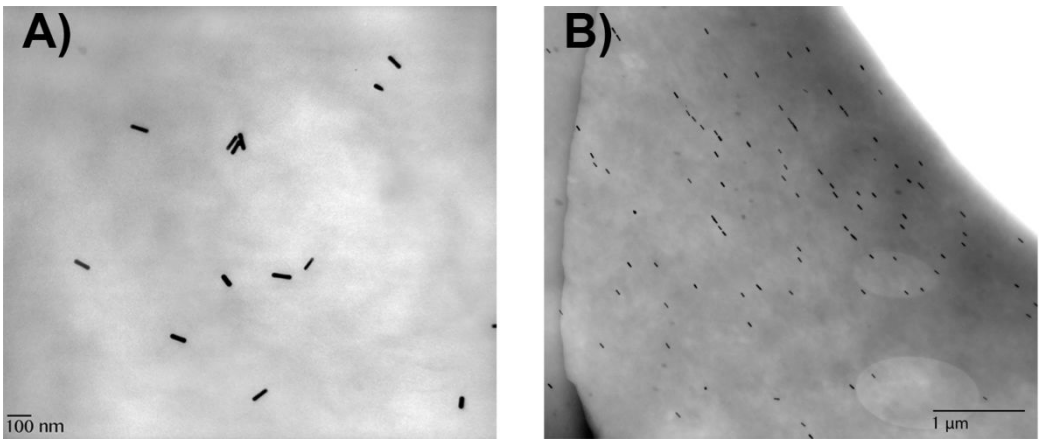

Figure 9: Transmission electron microscopy images of 2.0 nM PEG-SH AuNRs in Na-alginate/PAAm hydrogels. (A) Unstretched hydrogel, magnification 40,000x (scale bar on image). (B) Stretched hydrogel, magnification 15,000x (scale bar on image).

4. CONCLUSIONS

In summary, the successful alignment of gold nanorods with stretchable alginate/PAAm hydrogels was achieved. It was found that the modulus remains unchanged for Na-alginate/PAAm hydrogels for low concentration of AuNR as compared to the hydrogel without

Soft Matter

any AuNRs. However, at higher concentrations of AuNR the modulus decreases more than 25%. For Ca-alginate/PAAm, the surface chemistry also has an effect as the native hydrogel without AuNRs has a modulus of 64 ± 18 kPa and the modulus is decreased to 38 ± 6 kPa for hydrogels containing CTAB AuNRs. This surface chemistry impact is also observed when determining the maximum elongation of the Na-alginate/PAAm hydrogels, as the hydrogels containing MUA AuNRs had an increased stretchability, more than 3,000% its initial length. Using polarized UV-vis spectroscopy and TEM, AuNR alignment was observed when the hydrogel was stretched for all AuNR concentrations and surface chemistries tested. The AuNRs became more aligned along the stretch direction as the hydrogel was stretched further, with complete alignment along the stretch direction when the hydrogel was stretched around 400% its initial length. This work shows the influence nanoscale level properties can have on bulk mechanical properties of multi-component polymer composites and demonstrates the ability to align AuNRs in a biocompatible hydrogel.

ASSOCIATED CONTENT

Supporting Information.

S.I. contains characterization of gold nanorods and the functionalization process, raw data for mechanical measurements, ATR-FTIR of hydrogels, and polarized UV-vis measurements for each type of hydrogel.

AUTHOR INFORMATION

Corresponding Author

*Email: murphycj@illinois.edu

Soft Matter

ORCID

Jacob G. Turner: 0000-0001-6687-1536

Jun Hyup Og: 0000-0002-4631-0413

Catherine J. Murphy: 0000-0001-7066-5575

Author Contributions

†These authors contributed equally.

Notes

The authors declare no competing financial interest.

ACKNOWLEDGMENTS

The authors thank the National Science Foundation for its support of this work under CHE-1608743. The authors thank Dr. Hyunjoon Kong and his students for the training and usage of their 1 kN MTS Insight 2 tensile instrument. Special thanks to Lou Ann Miller for her help with imagining the AuNR hydrogels in TEM and preparing the samples. DMA and TEM was performed in the Frederick Seitz Materials Research Laboratory Central Research Facilities, University of Illinois at Urbana-Champaign.

Soft Matter

REFERENCES

1 J. P. Gong, *Soft Matter*, 2010, **6**, 2583–8.

2 A. Vedadghavami, F. Minooei, M. H. Mohammadi, S. Khetani, A. R. Kolahchi, S. Mashayekhan and A. Sanati-Nezhad, *Acta Biomaterialia*, 2017, **62**, 42–63.

3 Q. Chen, H. Chen, L. Zhu and J. Zheng, *Journal of Materials Chemistry B*, 2015, **3**, 3654–3676.

4 X. Zhang, B. Lin, K. Zhao, J. Wei, J. Guo, W. Cui, S. Jiang, D. Liu and J. Li, *Desalination*, 2015, **365**, 234–241.

5 M. C. Echave, R. M. A. Domingues, M. Gómez-Florit, J. L. Pedraz, R. L. Reis, G. Orive and M. E. Gomes, *ACS Appl. Mater. Interfaces*, 2019, **11**, 47771–47784.

6 S. Xie, B. Ren, G. Gong, D. Zhang, Y. Chen, L. Xu, C. Zhang, J. Xu and J. Zheng, *ACS Applied Nano Materials*, 2020, **3**, 2274–2786.

7 H. Liu, M. Li, C. Ouyang, T. J. Lu, F. Li and F. Xu, *Small*, 2018, **14**, 1801711–9.

8 J. Chen, Q. Peng, T. Thundat and H. Zeng, *Chem. Mater.*, 2019, **31**, 4553–4563.

9 H. Haider, C. H. Yang, W. J. Zheng, J. H. Yang, M. X. Wang, S. Yang, M. Zrínyi, Y. Osada, Z. Suo, Q. Zhang, J. Zhou and Y. M. Chen, *Soft Matter*, 2015, **11**, 8253–8261.

10 J.-Y. Sun, X. Zhao, W. R. K. Illeperuma, O. Chaudhuri, K. H. Oh, D. J. Mooney, J. J. Vlassak and Z. Suo, *Nature*, 2012, **489**, 133–136.

11 Q. Rong, W. Lei and M. Liu, *Chem. Eur. J.*, 2018, **24**, 16930–16943.

12 S. Talebian, M. Mehrali, N. Taebnia, C. P. Pennisi, F. B. Kadumudi, J. Foroughi, M. Hasany, M. Nikkhah, M. Akbari, G. Orive and A. Dolatshahi-Pirouz, *Adv. Sci.*, 2019, **43**, 1801664–47.

13 M. J. A. Hore and R. J. Composto, *Macromolecules*, 2014, **47**, 875–867.

14 H. Koerner, J. Kelley, J. George, L. Drummy, P. Mirau, N. S. Bell, J. W. P. Hsu and R. A. Vaia, *Macromolecules*, 2009, **42**, 8933–8942.

15 M. Moniruzzaman and K. I. Winey, *Macromolecules*, 2006, **39**, 5194–5205.

16 C. J. Ward, R. Tonndorf, A. Eustes, M. L. Auad and E. W. Davis, *Journal of Nanomaterials*, 2020, **2020**, 1–8.

17 C. J. Murphy and C. J. Orendorff, *Adv. Mater.*, 2005, **17**, 2173–2177.

Soft Matter

18 L. Dai, X. Lu, L. Song, Y. Huang, B. Liu, L. Zhang, J. Zhang, S. Wu and T. Chen, *Adv. Mater. Interfaces*, 2018, **5**, 1800026.

19 J. Pérez-Juste, B. Rodríguez-González, P. Mulvaney and L. M. Liz-Marzán, *Adv. Funct. Mater.*, 2005, **15**, 1065–1071.

20 B. M. I. van der Zande, L. Pagès, R. A. M. Hikmet and A. van Blaaderen, *J. Phys. Chem. B*, 1999, **103**, 5761–5767.

21 H. Pletsch, M. Tebbe, M. Dulle, B. Förster, A. Fery, S. Förster, A. Greiner and S. Agarwal, *Polymer*, 2015, **66**, 167–172.

22 K. Yang, Q. Han, B. Chen, Y. Zheng, K. Zhang, Q. Li and J. Wang, *IJN*, 2018, **13**, 2217–2263.

23 M. C. Arno, M. Inam, A. C. Weems, Z. Li, A. L. A. Binch, C. I. Platt, S. M. Richardson, J. A. Hoyland, A. P. Dove and R. K. O'Reilly, *Nature Communications*, 2020, **11**, 1420.

24 A. K. Gaharwar, N. A. Peppas and A. Khademhosseini, *Biotechnology and Bioengineering*, 2013, **111**, 441–453.

25 P. Thoniyot, M. J. Tan, A. A. Karim, D. J. Young and X. J. Loh, *Adv. Sci.*, 2015, **2**, 1400010.

26 N. D. Burrows, W. Lin, J. G. Hinman, J. M. Dennison, A. M. Vartanian, N. S. Abadeer, E. M. Grzincic, L. M. Jacob, J. Li and C. J. Murphy, *Langmuir*, 2016, **32**, 9905–9921.

27 H. Chen, L. Shao, Q. Li and J. Wang, *Chem. Soc. Rev.*, 2013, **42**, 2679–2724.

28 M. Keshavarz, K. Moloudi, R. Paydar, Z. Abed, J. Beik, H. Ghaznavi and A. Shakeri-Zadeh, *J Biomater Appl*, 2018, **33**, 161–169.

29 A. Roth, F. Murschel, P.-L. Latreille, V. A. Martinez, B. Liberelle, X. Banquy and G. De Crescenzo, *Biomacromolecules*, 2019, **20**, 1926–1936.

30 P. Baei, S. Jalili-Firoozinezhad, S. Rajabi-Zeleti, M. Tafazzoli-Shadpour, H. Baharvand and N. Aghdami, *Materials Science & Engineering C*, 2016, **63**, 131–141.

31 M. Shevach, S. Fleischer, A. Shapira and T. Dvir, *Nano Lett.*, 2014, **14**, 5792–5796.

32 E. M. Grzincic and C. J. Murphy, *ACS Nano*, 2015, **9**, 6801–6816.

33 C.-L. Zhang, F.-H. Cao, J.-L. Wang, Z.-L. Yu, J. Ge, Y. Lu, Z.-H. Wang and S.-H. Yu, *ACS Appl. Mater. Interfaces*, 2017, **9**, 24857–24863.

Soft Matter

34 S. R. Sershen, G. A. Mensing, M. Ng, N. J. Halas, D. J. Beebe and J. L. West, *Adv. Mater.*, 2005, **17**, 1366–1368.

35 I. Pastoriza-Santos, C. Kinnear, J. Perez-Juste, P. Mulvaney and L. Liz-Marzan, *Nature Reviews Materials*, 2018, **3**, 375–391.

36 M. G. Arafa, R. F. El-Kased and M. M. Elmazar, *Sci Rep*, 2018, **8**, 13674.

37 C. Ghisleri, M. Siano, L. Ravagnan, M. A. C. Potenza and P. Milani, *Laser & Photonics Reviews*, 2013, **7**, 1020–1026.

38 J. Wen, H. Zhang, H. Chen, W. Zhang and J. Chen, *J. Opt.*, 2015, **17**, 114015.

39 J.-E. Lee, C. Park, K. Chung, J. W. Lim, F. Marques Mota, U. Jeong and D. H. Kim, *Nanoscale*, 2018, **10**, 4105–4112.

40 A. M. Alkilany, L. B. Thompson and C. J. Murphy, *ACS Appl. Mater. Interfaces*, 2010, **2**, 3417–3421.

41 C. H. Yang, M. X. Wang, H. Haider, J. H. Yang, J.-Y. Sun, Y. M. Chen, J. Zhou and Z. Suo, *ACS Appl. Mater. Interfaces*, 2013, **5**, 10418–10422.

42 L. Vigderman and E. R. Zubarev, *Chem. Mater.*, 2013, **25**, 1450–1457.

43 J. G. Hinman, J. G. Turner, D. M. Hofmann and C. J. Murphy, *Chem. Mater.*, 2018, **30**, 7255–7261.

44 A. S. D. S. Indrasekara, R. C. Wadams and L. Fabris, *Part. Part. Syst. Charact.*, 2014, **31**, 819–838.

45 M. J. Hore and R. J. Composto, *Current Opinion in Chemical Engineering*, 2013, **2**, 94–101.

46 M. S. Islam, R. Masoodi and H. Rostami, *Journal of Nanoscience*, 2013, **2013**, 275037.

47 M. H. Pol and G. H. Liaghat, *Polym. Compos.*, 2015, **38**, 205–212.

48 P. Demianenko and B. Minisini, *J Chem Eng Process Technol*, 2016, **7**, 1000304.

49 J. Yang, C.-R. Han, F. Xu and R.-C. Sun, *Nanoscale*, 2014, **6**, 5934–10.

50 P. K. Jain and M. A. El-Sayed, *Chemical Physics Letters*, 2010, **487**, 153–164.

Soft Matter

TOC Figure